DOI:10.28974/idojaras.2024.3.4

IDŐJÁRÁS

Quarterly Journal of the HungaroMet Hungarian Meteorological Service
Vol. 128, No. 3, July – September, 2024, pp. 345–366

The influence of rural areas transformation on the urban heat islands occurrence – Tourist center Zlatibor case study

Ljiljana Mihajlović [1, *], **Ivan Potić** [2], **Miroljub Milinčić** [3], and **Dejan Đorđević** [4]

[1] *Faculty of Geography, University of Belgrade*
Belgrade, Serbia

[2] *Military Geographical Institute "General Stevan Bošković"*
Belgrade, Serbia

[3] *Faculty of Geography, University of Belgrade*
Belgrade, Serbia

[4] *Military Geographical Institute "General Stevan Bošković"*
Belgrade, Serbia

* *Corresponding Author E-mail: ljiljana.mihajlovic@ gef.bg.ac.rs*

(Manuscript received in final form August 4, 2023)

Abstract— As urbanization continues to increase, changes in the ecological characteristics of urban areas are becoming more reasonable to meet the needs of a growing population. However, the profound impact of human-induced urban pressures on land, often called the "billing impact", is strongly emphasized in research publications. In many cases, contemporary anthropogenic processes alter the dynamics of environmental functions in complex ways. Urban regions meet a particular climate regime characterized by increased air temperatures compared to peripheral areas and a significant reduction in wind speed, attributable to the interaction of natural and anthropogenic factors. An urban heat island (UHI) occurs when the air above populated areas heats up additionally, causing air to flow from the site's edges to its center and creating a heat dome. This study reveals the influence of urbanization on microclimatic changes, encompassing increased evapotranspiration, altered vegetation cover, and temperature fluctuations. The results illustrate environmental transformations caused by abrupt and unregulated urbanization in the mountainous area of Zlatibor, Serbia, a trend that has intensified over the past decade.

Key-words: image analysis, GIS analysis, landsat, multispectral imagery, thermal infrared bands, land surface temperature, actual evapotranspiration

1. Introduction

Urbanization presents activities to enhance underdeveloped urban regions or create new infrastructure in undeveloped areas. The primary objective of these activities is to provide enhanced quality of life for the population. These processes frequently lead to a shift in the operational dynamics of the settlements. Contemporary society and lifestyle demands drive the significant conversion of nature, especially vegetated areas (*Grădinaru et a*l., 2020; *Tosic* and *Obradovic*, 2003). The interaction between nature and society forms an organically linked system, with the ecological characteristics of the resulting urbiocoenoses primarily determined by the degree of artificial pressure exerted on nature in urbanized regions. Such characteristics distinguish them from the original biogeocoenoses. As the biosphere transforms into the biotechnosphere, it becomes crucial to study one of the most significant thermodynamic characteristics of the biosphere and its components (*Vukoičić et al.*, 2023). The community's social organization and the effective management of social processes influence urbanization's pace, form, and characteristics. Urbanization is a process characterized by a substantial aggregation of activities within regions designated for priority development (*Živanović et al*., 2021). One of the vital material outcomes of modern urbanization is the creation of vast urban regions, a conglomeration of interconnected suburban villages, forming a complex dynamic system.

Zlatibor Mountain is a popular tourist destination within the Dinaric Alps Mountain range in the western part of Serbia. Famous for its green forests, pristine rivers, and attractive landscapes, the mountain of Zlatibor serves as a sanctuary for those who appreciate the natural world and engage in outdoor pursuits. It provides a multitude of opportunities for activities including, but not limited to, hiking, skiing, cycling, and fishing (*Pecelj et al.*, 2017). Furthermore, with its attractive natural features and traditional values combined with modern urban development trends, Zlatibor Mountain is an area that urbanizes remarkably quickly and is an exceptional subject for this study.

The study and understanding of the surface urban heat island (SUHI) have far-reaching implications across various fields. In climatology, it helps us understand the impact of urbanization on local and global climate patterns (*Zhou et al.*, 2015). In geography, it aids urban planning and the development of strategies to mitigate heat-related health risks (*Tan et al*., 2010). In tourism, SUHI influences tourist behavior and preferences, potentially impacting the local economy (*Zhou et al.*, 2016). Researchers extensively study the SUHI phenomenon using remote sensing technology, which provides a comprehensive spatial and temporal understanding of UHIs (Zhou et al., 2016). For instance, satellite data enables the quantification of SUHI effects across various urban forms and climatic conditions (*Zhou et al.*, 2014). The rise in global urbanization and its associated environmental and health challenges highlight the importance

of SUHI research. Therefore, it continues to be a crucial study area in urban climatology and related fields.

Researchers can study the UHI-derived phenomena by analyzing the air temperature observed at urban and rural weather stations and using land surface temperature data obtained through remote sensing (*Imhoff et al*., 2010). However, studying the UHI phenomenon in regions with insufficient weather stations can be challenging. With its extensive area synchronization and spatial coverage advantages, remote sensing data has become an effective tool for studying the UHI phenomenon (*Gallo et al*., 1993; *Gong et al.*, 2008; *Weng et al.*, 2004). The first use of the infrared thermal band from satellite imagery to study the UHI effect occurred in 1972 (*Rao*, 1972). Since then, remote sensing data and algorithms have been utilized and improved to examine the UHI effects (Cao et al., 2016; *Liu* and *Li*, 2018; *Stathopoulou* and *Cartalis*, 2007; *Tang et al.*, 2022). Analyses have been conducted on the scale of UHI phenomena and its spatiotemporal evolution features, considering its implications on diverse environmental factors. Additionally, researchers actively search for measures to mitigate its harmful effects (Chen et al., 2016; *Imhoff et al.*, 2010; *Priyadarsini et al*., 2008; *Stathopoulou* and *Cartalis*, 2007; *Streutker*, 2003; *Voogt* and *Oke*, 2003).

The formation of "heat islands" has several effects: a decrease in relative and absolute humidity, the emergence of a rising convection current, a decrease in wind speed, an increase in cloud cover and precipitation, an increase in the frequency of smog-like fog, and a decrease in solar radiation (*Mohajerani et al.,* 2017; *Pecelj et al.*, 2021). In addition to measuring the temperature of a given area, estimates of evapotranspiration (ETa) derived through remote sensing and global weather datasets provide valuable information about the existence of UHI. Such information proves useful for various applications, including calculating a basin's water budget, evaluating water consumption and crop yield, and monitoring drought conditions. The process of evapotranspiration is essential to understand the energy and water budgets of the planet, in addition to the carbon cycle. Acquiring a time series of spatially consistent, historical Landsat data for the entire world is a significant step forward in advancing scientific knowledge (*Sugiarto et al.*, 2021).

Heat domes, rarely exceeding 700 meters in height, intensify air pollution in cities and populated areas (*Lješević* and *Mihajlović*, 2020). Its distribution and strength depend on the size of the city, the area it occupies, the density of buildings, variations in air temperature and humidity, and differences in land use. The wind regime affects the extent and shape of the heat dome above the surface. At wind speeds between 10 and 15 m/s, a dome cannot exist (*Mohajerani et al*., 2017). Therefore, a wind of this speed cleans the air during the day more effectively than 20 times the air exchange (*Pecelj et al.*, 2010; 2017). However, even under these conditions, the dome can become a cloud of air pollution covering suburban areas (settlements, recreational areas, agricultural land, and others).

This study aims to delve into the impact of urbanization on the UHI and SUHI effects, with a particular emphasis on the Zlatibor Mountain region. Zlatibor Mountain, situated in the southwestern region of Serbia, extends from northwest to southeast, covering a vast area of approximately 1.015 km². It spans 55 km in length and 22 km in width, encompassing significant portions of the widespread Starovlaška plateau. The mountain shares its borders with the Kremna Valley to the northwest, the Sušica and Mačkatska areas to the north, the Murtenica Mountain to the southeast, and the Uvac River to the south. Additionally, a foothill connecting to Tara also forms a part of Zlatibor. Located at a distance of 230 km from the Serbian capital of Belgrade (*Fig. 1*), Zlatibor Mountain is accessible via the Zlatibor magisterial road, which serves as a crucial route connecting Belgrade to the Adriatic Sea coast.

Regarding tourism, Zlatibor is predominantly known for its central part – a spacious rolling plateau, about 30 km long and 12 km wide. Several peaks and tops, including Tornik, Čigota, Gradina, Čavlovac, Viogor, Crni Vrh, and the upper stream of the Sušica River, border this central area (*Stojsavljević et al.*, 2016). The research uses remote sensing data and other relevant datasets to analyze the changes in land surface temperature and evapotranspiration rates and their implications on the local climate and environment. The findings from this study enrich the growing body of knowledge on UHI, and provide valuable insights for urban planning and environmental management in the face of rapid urbanization.

2. Materials and methods

2.1. Study area

The initial hypothesis of this article is that the urban heat islands have emerged after intensive and excessive construction in the tourist center of Zlatibor. This tourist center, located in the western part of Serbia, is near Užice (*Fig. 1a*) and Čajetina town (*Fig. 1c*). The study area includes the surrounding area of the newly built urban environment in the tourist center (according to the 2022 situation). The study area extends to 4,847,038.68 m N, 391,257.58 m E, and 4,838,842.59 m N, 399,385.45 m E (*Fig. 1b*) and covers an area of 66.62 km^2. The urban part of the study area covers an area of 9.48 km^2 with a mean geographic center at 4,842,793.46 m N and 395,452.68 m N. The UTM34N projection provides all coordinates.

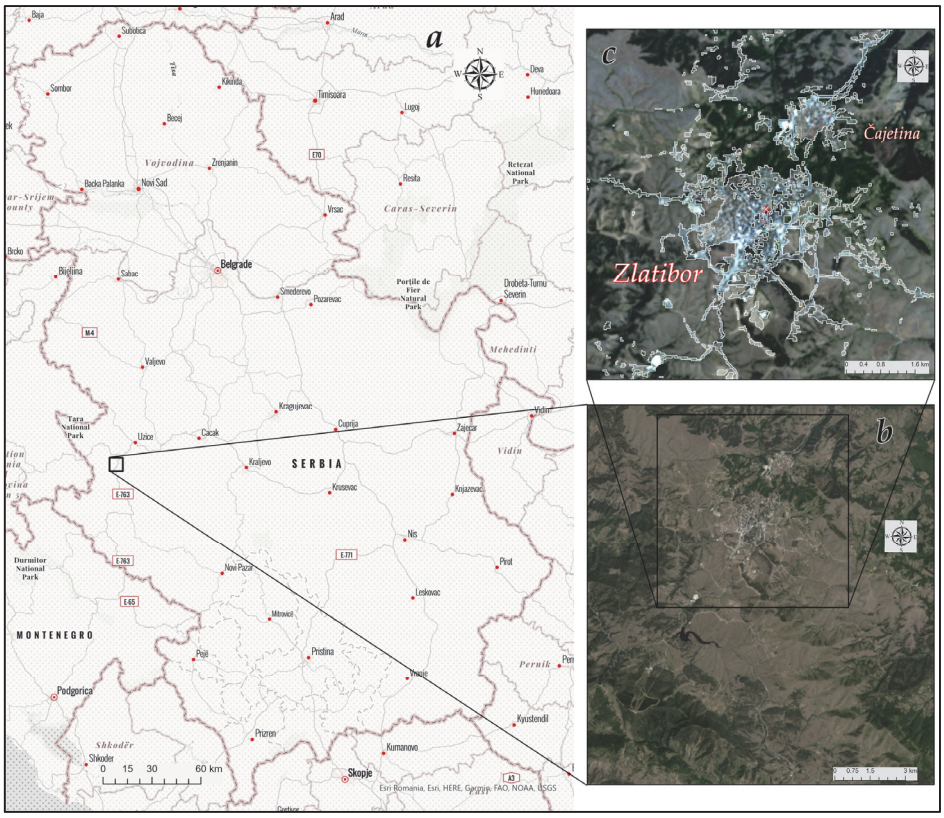

Fig. 1. Zlatibor's a) position within Serbia, b) the Area area of interest (AOI), c) urban part of AOI.. (*Engebretson*, 2020a; *Prostak*, 2023)

The tourist center of Zlatibor has undergone substantial urbanization, particularly in developing tourism infrastructure, over the past three decades. The region witnesses growth in hotels, restaurants, cafes, and other amenities, enhancing its appeal as a tourist destination (*Basarin et al*., 2018). This area lacks regulated urbanization, with individual houses making up most of the permanent residential space. However, collective housing is available in the tourist center of Zlatibor and in the municipal headquarters. The main issue is the high prevalence of temporary residences such as weekend houses and holiday homes. The 2011 census data reveals that the area contains 7,229 permanent and temporary dwellings, covering 637,182 m^2. The municipality undergoes the construction of approximately 654 new apartments annually, spanning a total area of 33,714 m^2. Owing to the high rate of residential construction, the number of built apartments per 1,000 inhabitants has experienced a steady increase since 2015 (*Republički zavod za statistiku Srbije*, 2023). This extensive and unregulated construction exerts significant pressure on the environment, while simultaneously, urbanization brings new job opportunities and stimulates economic growth in the region. Nevertheless, it has also upraised concerns about the impact of tourism on the environment, including waste management, water supply, and air temperature

increase. Despite these challenges, Zlatibor Mountain remains a popular tourist destination, combining natural beauty and modern amenities. The region continues to attract visitors from all over the world, seeking relaxation, outdoor activities, and a taste of Serbian culture.

Zlatibor's geological structure primarily consists of Zlatibor ultramafites, the Triassic sediments, and ophiolitic mélange in the eastern part of the area (*Dimitrijević,* 1996). Tertiary formations cover this area in some places, with a thin rim of Paleozoic bedrock. The Zlatibor Mountain area is part of the ophiolitic zone of the inner Dinaric Alps belt (*Vakanjac et al*., 2015). It is made up of Paleozoic phyllites, sandstones, and conglomerates, as well as Mesozoic rocks of the diabase-rose stone formation. Palaeozoic rocks comprise most of the geological structure, while Neogene sediments have been formed on land once inhabited by lakes.

The climate is moderately continental in the low, northern part of the region, but becomes sub-mountainous as altitude ascends. The average summer air temperature is about 25 °C, while winter air temperatures can drop to -5 °C. The yearly precipitation typically ranges between 700 and 900 millimeters (*Novković*, 2008).

The land cover of the study area presents a mix of barren, developed, forest, and herbaceous regions, with a minimal proportion of water bodies based on 2022 data (*Table 1*). The dominance of barren and developed lands may underscore prevailing environmental and anthropogenic factors influencing the landscape. Barren land is the most prominent class, covering most of the area. This category, often signifying a scarcity of vegetation, covers a substantial 52.16% of the total study area. The prominent presence of barren land suggests potentially harsh or unproductive environmental conditions. The second most widespread class is developed land, approximately 14.24% of the total study area. This classification typically refers to areas with a considerable human footprint, such as settlements, infrastructures, or extensively cultivated lands. The proportion of developed land might signal significant human activity or industrial influence. Forest and herbaceous classes encompass relatively similar areas. Forest land, indicative of areas dominated by trees and other woody plants, occupies 17.93% of the study area. However, herbaceous land, usually characterized by grasses, herbs, and other non-woody plants, accounts for 15.59% of the total study area. The presence of these classes suggests a balance of both woody and non-woody vegetated zones in the study area. Finally, the smallest class (water land), represents a minuscule 0.08% of the total study area. This diminutive portion implies that surface water bodies like lakes, rivers, or reservoirs are likely scarce within the study area.

Identifying and mapping UHI requires multiple inputs (*Fig. 2*). The process begins with analyzing meteorological data to verify the temperature change hypothesis and determine the critical point at which this phenomenon emerged. The next step involves scrutinizing satellite images and their related outputs (*Fig. 2*) for more precise information.

2.2. Meteorological data

The air temperature data used to create a database for this research are collected from meteorological statistical yearbooks of the Hydrometeorological Service of the Republic of Serbia for the Zlatibor meteorological station and the given climatological period. The research encompassed a complete climatological cycle of at least a 30-year time series and followed the World Meteorological Organization (WMO) guidelines.

From 1986 to 2022, air temperature (RHSS, 1987–2022) change is analyzed to determine the trend of mean August values and the threshold year, in which the mean monthly air temperature did not drop below 16 °C.

August is chosen as the warmest month of the year in the meteorological station Zlatibor, located within the settlement of Zlatibor at an altitude of 1,029 m.a.s.l. (RHSS, 1987–2022).

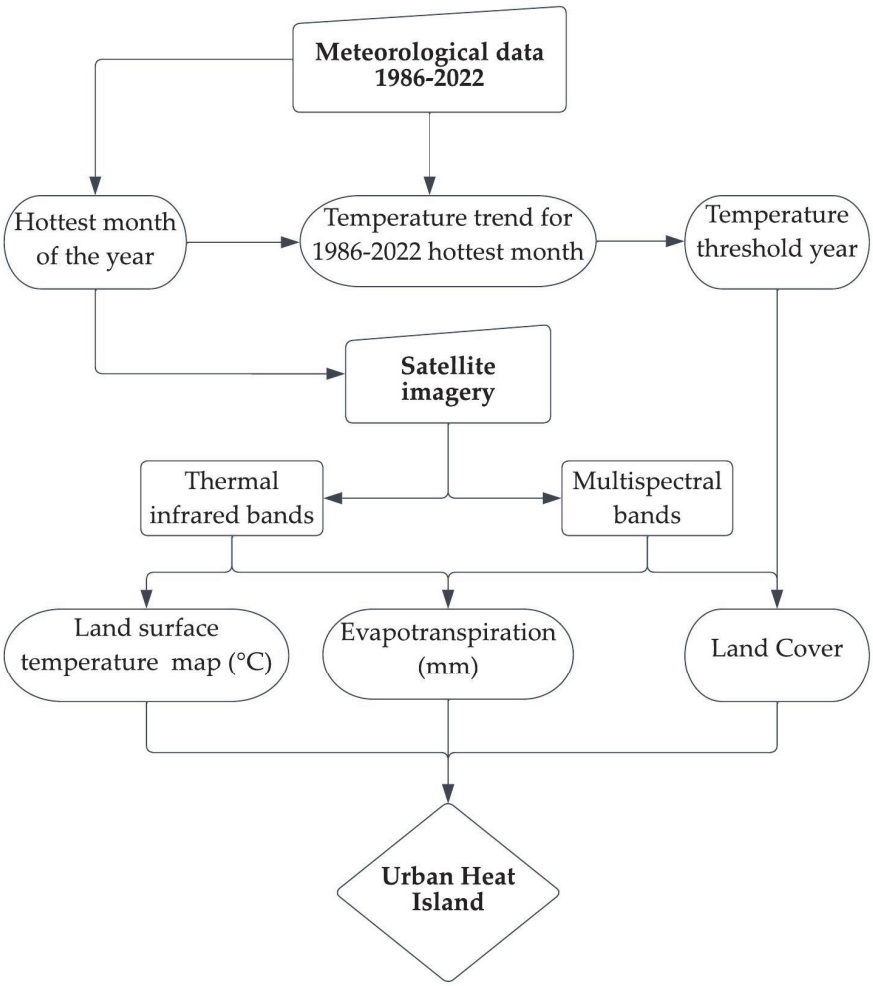

Fig. 2. Flow chart of urban heat island detection used in this research.

2.3. Satellite imagery processing

The creation of Landsat Level-2 science products involves using Collection 2 Level-1 inputs that do not exceed the 76 degrees Solar Zenith Angle limitation and include the necessary auxiliary input data to provide a scientifically credible solution (*Sayler et al*., 2022; *Sayler* and *Zanter*, 2021). The Version 1.5.0 of the Land Surface Reflectance Code (LaSRC) algorithm generates the Landsat 8/9 Operational Land Imager (OLI) surface reflectance products. (*Engebretson*, 2020a). The Landsat 4–5 surface reflectance products are created using the Version 3.4.0 Landsat Ecosystem Disturbance Adaptive Processing System (LEDAPS) algorithm (*Engebretson*, 2020b). The Landsat 4-9 surface temperature products are produced using the Landsat surface temperature algorithm Version 1.3.0, created in collaboration with NASA's Jet Propulsion Laboratory and Rochester Institute of Technology (*Cook*, 2014).

Land surface temperature (*LST*) products are measured in Kelvin (K) and generated with a 30-meter spatial resolution. Landsat Collection 2 Level-1 thermal infrared bands, TOA Reflectance, TOA Brightness temperature, ASTER Global Emissivity Database (GED) data, ASTER NDVI, and atmospheric profiles of geopotential height, specific humidity, and air temperature obtained from ASTER data are used to produce Landsat Level-2 Surface Temperature products (*Sayler et al*., 2022). The final step is to calculate the *LST* in °C (*Avdan* and *Jovanovska*, 2016):

$$LST = BT / \{1 + [(\lambda BT / \rho) \ln (LS\varepsilon)]\} \ , \qquad (1)$$

where BT is at-sensor brightness temperature in °C, λ is the wavelength of emitted radiance (center wavelengths for Landsat TIR bands are: for Landsat 5 Band 6 value is 11.45, and for Landsat 8 Bands 10 and 11 values are 10.895 and 12, respectively (*Engebretson*, 2020b; *Sayler et al*., 2022)), $LS\varepsilon$ is the emissivity, and ρ is the density of air.

The amount of water vaporising from a surface due to evaporation and transpiration is called actual evapotranspiration (*ETa*), measured in millimetres (mm). ETa is derived from the Landsat Level-2 Surface Temperature products and uses a scene-based approach. The Landsat Surface Temperature is one of the variables provided in a surface energy balance model, along with other auxiliary data, to calculate the daily total of *ETa*, which is part of the product entitled Landsat Collection 2 Level-3 Provisional Actual Evapotranspiration Science (*Sayler* and *Glynn*, 2022). The robust model solves the surface energy balance equation for the latent heat flow to produce the Landsat C2 Provisional *ETa* products. This *ETa* computation uses a surface energy balance model built directly from the Operational Simple Surface Energy Balance (SSEBop) model (*Senay*, 2018; *Senay et al*., 2013, 2022, 2023). An SSEBop model is provided with

the Landsat C2 Level-2 Surface Temperature product and external auxiliary data to derive the daily total of *ETa.*

The SSEBop model is a parametric energy balance-based model that considers real *ET* to be the product of two independently estimated quantities: (1) *ET* fraction (*ETf*) and (2) the maximum *ET* under water-unlimited environmental circumstances *(ETr*) (*Senay et al*., 2023):

$$ETa = ETf \cdot ETr, \tag{2}$$

where *ETa* is the actual *ET* (mm) and *ETr* is the alfalfa-reference ("maximum/potential") *ET* (mm).

Land cover classification uses Landsat 5 and Landsat 8 (*Sayler* and *Zanter*, 2021) optical bands. Imagery from 3 different periods (initial 1986, threshold 2005, and final 2022) is acquired using USGS Earth Explorer (*U.S.G.S*., 2015) application. Five different classes are distinguished: 1) water, 2) developed, 3) forest, 4) herbaceous, and 5) barren land. Class "water" includes areas of open water, such as lakes, rivers, and ponds. Class "developed" includes areas developed for human use, such as residential, commercial, and industrial areas, and includes transportation infrastructure, such as roads, airports, and railroads. Class "Forest" includes areas dominated by trees (natural or planted forests). Forests can include a variety of tree species. The "herbaceous" class refers to areas dominated by non-woody plants, such as grasslands, fields, lawns, or other open areas. These areas may be natural or managed landscapes like parks or lawns. The "barren land" class refers to landscape areas with little to no plant life. This class could include deserts, rocks, sand, or other areas, where the soil is too poor to support much plant life. These areas are often devoid of human activity due to their harsh conditions. SVM classifier is employed in semi-automatic supervised object-based classification procedures using ArcGIS Pro (*Esri Inc*., 2023) to perform satellite image classification and obtain a land cover map for a specific year.

The SUHI effect is a significant environmental concern characterized by higher temperatures in urban areas than in rural ones. Human activities, urbanization, and modifying natural landscapes cause this phenomenon. The quantification of the SUHI effect is typically achieved by subtracting the rural temperature from the urban temperature (*Zhou et al.*, 2014), and in recent years, there have been several advancements in the methodologies used to study and mitigate the SUHI effect (*Almeida et al.,* 2022; *Bande et al*., 2022; *Fardani* and *Yosliansyah*, 2022).

3. Results

Fig. 3 presents the analysis of average August air temperatures over 37 years, from 1986 to 2022. The trendline reveals a consistent rise in these air temperatures. The data exhibits yearly variability, with the highest average temperature recorded in 2012 (21.00 °C) and the lowest in 1995 (15.40 °C). Some years, such as 1992, 1994, 2000, 2003, 2012, 2015, 2017, and 2019, have air temperatures above the average, while others, like 1987, 1991, 1995, 1997, 2002, 2005, and 2016, fall below the average.

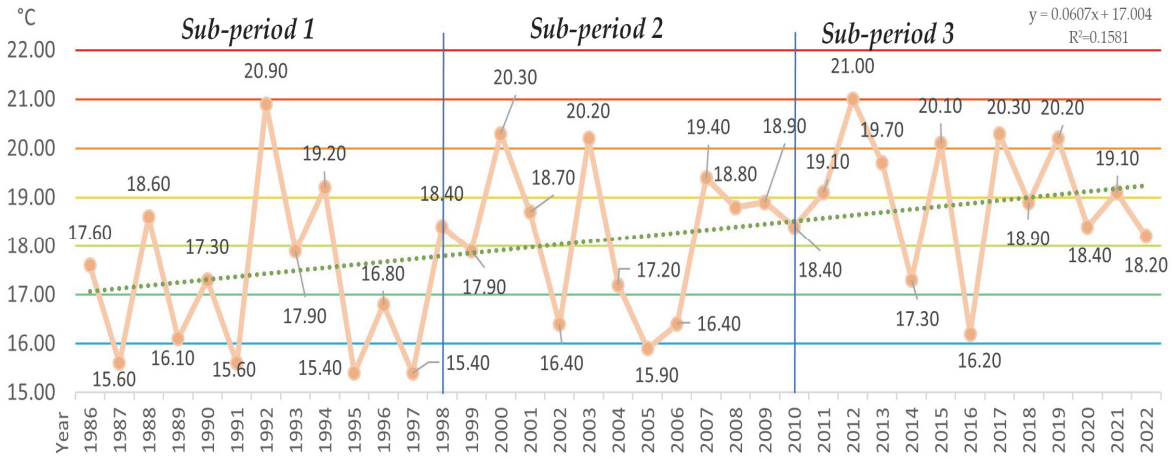

Fig. 3. Average August air temperatures (°C) in the period 1986–2022.

Overall, the data suggest some variability in August air temperatures from year to year, but the average air temperature over the 37 years is 17.96 °C.

Empirically, the air temperature data indicates that 2005 is a temperature threshold year suitable to present the studied area's mean urbanization state related to the temperature increase. The temperature threshold year is chosen by dividing the thirty-seven-year observation period into three sub-periods to compare the lowest monthly average temperatures (*Fig. 3*). The data shows that 2005 is the last year with an average monthly temperature below 16 °C. The given linear trend equation, $y = 0.0607x + 17.004$, indicates a positive linear relationship between the years (independent variable, x) and the average monthly air temperature in August (dependent variable, y) for the study area. The slope of the trend line (0.0607) suggests an annual increase in August air temperatures. Specifically, the average monthly air temperature for August tends to rise by approximately 0.0607 °C for each one-year increase. The equation suggests a long-term warming trend over the observed period, despite potential fluctuations from year to year. Thus, the evidence supports the assertion that there is an increasing trend in the August air temperatures for the observed period and study area. However, the coefficient of determination, $R^2 = 0.1581$, implies that

approximately 15.81% of the variance in the average monthly air temperature can be explained by the year in the context of this model. Therefore, a substantial portion of the variance (around 84.19%) is still unexplained by the linear model. This result suggests other factors influencing the average August air temperature beyond time (year). These factors could encompass various climatic or anthropogenic elements not accounted for in the simple linear model. R^2 of 0.1581 signifies that the model has successfully captured a significant portion of the variation in the data. It implies that a definite structure underlies the data, as elucidated by the model, even though the model does not account for a substantial portion of the variability.

The land cover classes information is provided in *Table 1* for three different years, 1986, 2005, and 2022, in terms of their areas and percentages for a wider study area (Figure 1c). *Table 1* shows that the class „developed" has increased its area significantly over time, with 9.48 km^2 in 2022, 4.68 km^2 in 2005, and 0.71 km^2 in 1986. Determined values compute the increasing trend between 1986 and 2022 for the class „developed". The calculated percentage increase is 1 233.8%.

Table 1. Land cover results for 1986, 2005, and 2022 for Zlatibor study area

Class name	Area 2022 (km^2)	2022 (%)	Area 2005 (km^2)	2005 (%)	Area 1986 (km^2)	1986 (%)
Water	0.05	0.08	0.01	0.02	0.02	0.03
Developed	**9.48**	**14.24**	**4.68**	**7.02**	**0.71**	**1.07**
Forest	11.94	17.93	9.97	14.98	15.15	22.75
Herbaceous	10.38	15.59	38.73	58.17	21.78	32.71
Barren	34.73	52.16	13.19	19.81	28.93	43.45
Total	**66.58**	**100.0**	**66.58**	**100.0**	**66.58**	**100.0**

The precise analysis of *LST* and *ETa* results includes only the area of Zlatibor's widest urbanization (*Fig 1c*, white outline) according to the 2022 classification (9.48 km^2), which are shown in *Table 2* and *3*.

The *LST* ranges from 15 °C to 40 °C. In 1986, the area covered at lower *LST* values, between 15 °C and 24 °C, is much smaller than in 2022, indicating a significant increase in urbanization or land use change. In 2022, most areas are covered by *LST* values between 27 °C and 35 °C.

In 2022, the most extensive part of the Zlatibor urban area (4.495 km^2) exhibits *ETa* values in the 2–3 mm range. The second most extensive area (2.646 km^2) presents *ETa* values of 1–2 mm, while the smallest area (0.009 km^2) shows ETa values greater than 4 mm. Conversely, in 1986, the most significant area (4.641 km^2) shows *ETa* values in the 2–3 mm range, and the second-largest area (3.159 km^2) presents *ETa* values in the 3–4 mm range.

Table 3 reveals that the area with ETa values in the 2–3 mm range is the largest in both 1986 and 2022, covering 4.641 km^2 and 4.495 km^2, respectively, indicating that this range of *ETa* values is the most frequent in the Zlatibor urban expansion area.

Table 3 also highlights that the area with *ETa* values in the 1–2 mm range expands from 1.527 km^2 in 1986 to 2.646 km^2 in 2022, suggesting an increase in vegetation cover in the Zlatibor urban expansion area, leading to higher evapotranspiration rates in this range.

Table 2. Land surface temperature coverage 1986–2022 for Zlatibor main urban area

Temperature (°C)	**Area 2022 (km^2)**	**Area 1986 (km^2)**
15	/	0.003
16	/	0.075
17	/	0.269
18	/	0.518
19	/	0.697
20	/	1.031
21	/	1.274
22	/	1.766
23	/	1.310
24	/	0.893
25	/	0.770
26	0.002	0.343
27	0.048	0.230
28	0.243	0.241
29	0.963	0.052
30	1.331	0.009
31	1.597	/
32	1.457	/
33	1.276	/
34	0.926	/
35	0.781	/
36	0.522	/
37	0.198	/
38	0.105	/
39	0.029	/
40	0.004	/
Total area	**9.482**	**9.482**

Table 3. Evapotranspiration coverage in the period 1986–2022 for Zlatibor urban expansion area

***ETa* range (mm)**	**Area 2022 (km^2)**	**Area 1986 (km^2)**
0–1	0.325	0.155
1–2	2.646	1.527
2–3	4.495	4.641
3–4	2.007	3.159
> 4	0.009	/
Total area	**9.482**	**9.482**

Nevertheless, it is fundamental to mention that the area with *ETa* values in the 0–1 mm range also increased from 0.155 km^2 in 1986 to 0.325 km^2 in 2022. This trend may indicate that there has been an increase in impervious surfaces in the Zlatibor urban expansion area, such as paved roads and buildings, which has reduced the amount of vegetation and soil moisture, resulting in lower rates of evapotranspiration in this range.

To determine the SUHI effect, the region surrounding the Zlatibor main urban area (MUA) is divided into five distinct zones (*Fig. 4* and *Table 4*):

Zone 1, which represents the main urban area of Zlatibor.

Zone 2, which encompasses an area of 100 m around Zone 1.

Zone 3 covers an area from 100 m to 300 m from Zone 1.

Zone 4 includes the area from 300 m to 500 m from Zone 1.

Zone 5 covers the area from 500 m to 1000 m from Zone 1.

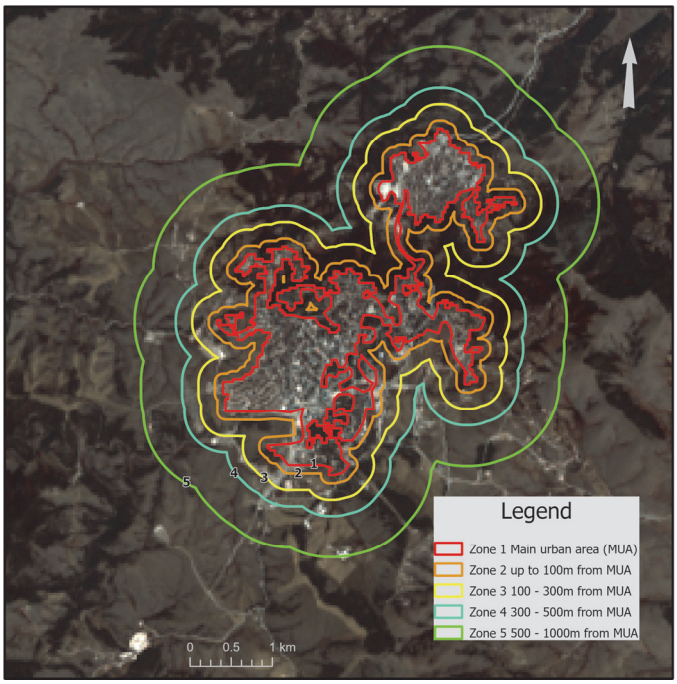

Fig. 4. Zlatibor's main urban area and buffer zones.

Table 4. Comparative analysis of air temperature variations in different zones of Zlatibor MUA from 1986 to 2022

Zone Id (2022)	MIN (2022)	MAX (2022)	RANGE (2022)	MEAN (2022)	STD (2022)	MEDIAN (2022)	Area km^2 (2022)
5	25.43	40.48	15.06	32.65	3.34	33.22	9.00
4	25.47	37.58	12.11	31.53	3.24	32.07	3.68
3	25.36	38.37	13.01	30.78	3.06	30.72	4.29
2	25.46	37.79	12.34	30.29	2.30	29.99	3.35
1	26.39	35.65	9.26	31.05	1.53	31.04	3.97
Zone Id (1986)	**MIN (1986)**	**MAX (1986)**	**RANGE (1986)**	**MEAN (1986)**	**STD (1986)**	**MEDIAN (1986)**	**Area km^2 (1986)**
5	14.25	29.18	14.94	22.35	3.29	22.82	9.00
4	13.78	29.18	15.40	20.81	3.22	21.06	3.68
3	14.25	29.18	14.94	20.07	3.02	20.17	4.29
2	14.25	26.25	12.00	19.76	2.39	19.73	3.35
1	15.18	27.93	12.76	21.13	2.24	21.06	3.97

In 2022, Zone 1, an urbanized area (*Fig. 5*), shows significantly higher *LST* values than the other zones. The mean temperature for Zone 1 is 31.05 °C, which is higher than the mean *LST* values of the other zones. This increase in *LST* is due to the SUHI effect, where urbanized areas tend to be warmer than their rural surroundings due to human activities and the physical characteristics of the built environment.

The minimum and maximum *LST* values for Zone 1 in 2022 are 26.39 °C and 35.65 °C, respectively, with a range of 9.26 °C. This range is the smallest among all zones, indicating a less variable *LST* within the urbanized area. The standard deviation, a measure of temperature variability, is also the lowest in Zone 1, further supporting this observation.

LST increases significantly in all zones, particularly in Zone 1, comparing the 2022 data with the 1986 data. The mean *LST* in Zone 1 increased from 21.13 °C in 1986 to 31.05 °C in 2022, a rise of nearly ten °C. This increase is more significant than those observed in the other zones, suggesting that urbanization has substantially impacted the *LST* rise. It is evident from the data that Zone 1, the most urbanised area, exhibits the highest mean *LST* in 2022 at 31.05 °C. This is a significant increase from the mean temperature of 21.13 °C recorded in 1986, underscoring the impact of urbanization on temperature rise.

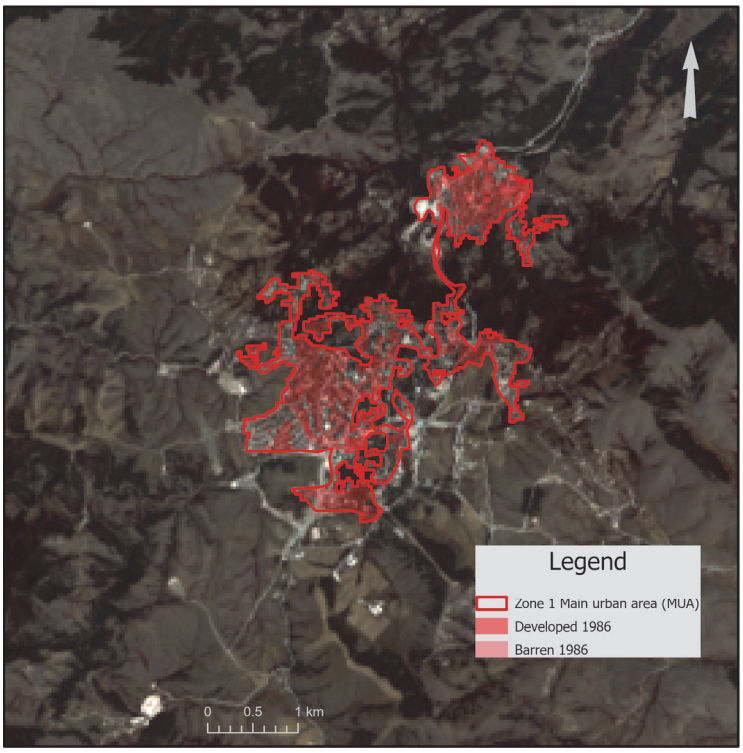

Fig. 5. Transformation of main urban area in Zlatibor: a dual temporal perspective of 1986 and 2022, highlighting urbanized and pre-urbanized land.

In contrast, Zones 2 to 5, which are less urbanized, show lower mean *LST* values in 2022. Specifically, Zone 2 has a mean LST of 30.29 °C, Zone 3 has 30.78 °C, Zone 4 has 31.53 °C, and Zone 5 has 32.65 °C. While high, the *LST* values for Zones 2 and 3 are still lower than the temperature in Zone 1, indicating that the level of urbanization directly correlates with the increase in temperature. The urbanization in Zone 1, characterized by increased building density and the transformation of natural landscapes into built environments, has led to a significant rise in the *LST* values. This change is a manifestation of the SUHI effect, where urbanized areas tend to be warmer than their rural surroundings due to human activities and the physical characteristics of the built environment. The built environment in Zone 1, with its concrete and asphalt structures, absorbs and retains heat more effectively than the natural landscape, increasing the ambient *LST*. This contrasts with Zones 2 to 5, where vegetation and rocks that absorb heat contribute to the high *LST* values, but not to the same extent as the urbanization in Zone 1. The data from the different zones in the Zlatibor settlement clearly illustrates the significant impact of urbanization on temperature rise. Despite the natural factors contributing to high LSTs in Zones 2 to 5, the effect of urbanization in Zone 1 is significantly more pronounced, leading to the highest mean *LST* among all zones. This underscores the need for sustainable urban planning strategies to mitigate the SUHI effect and promote thermal comfort in urban areas.

4. Discussion

The analysis of average August air temperatures over 37 years shows a constant increase in temperature from 1986 to the present, with some variability from year to year. The most deviant year is 2012, with the highest deviation from the mean. The data suggests that 2005 is a temperature threshold year, indicating increased urbanization and built-up areas. The area covered by class „developed" has increased dramatically over time, indicating rapid urbanization and development.

The tables also show an increase in temperature coverage in the higher temperature ranges, indicating the urban heat island effect and changes in the distribution of evapotranspiration ranges over time. Evapotranspiration values can provide valuable information about urban areas' water balance and environmental conditions. Urban areas often have a higher surface temperature than surrounding rural areas due to the urban heat island effect. This effect can increase the evapotranspiration rate in urban areas, as the higher temperature can increase the evaporation rate from the ground and plant transpiration. However, urban areas may also have lower vegetation and soil moisture levels than rural areas, which can decrease evapotranspiration rates. Additionally, human activities such as paving and building can alter the hydrological cycle, leading to changes in evapotranspiration rates (*Grimm et al.*, 2008).

One of the essential features of this process is the appearance of elements of the artificial environment in the study area: buildings, irrigation systems, transport, and other technical means of communication, which exert an increasing influence on the natural environment and change it, as it was already indicated earlier (*Vasilescu et al*., 2022). Urbanized regions have a dynamic interaction between the natural and artificial environments (biosphere and human-made structures), forming a distinct anthropogenic state of nature. This state, often referred to as the interface between nature and the built environment, is shaped by human actions and is profoundly influenced by our social nature. Overall, the data suggest a significant impact of human development on the environment in the study area.

The study has provided significant insights into the SUHI effect of the studied region. The results align with the findings of *Polydoros et al*. (2022), who also emphasized the role of landscape metrics in mitigating the SUHI effect. The current study's findings further substantiate this claim by providing empirical evidence from the studied region, thereby contributing to the existing body of knowledge on the subject.

However, the study diverges from the work of *Kiran* (2021), which focused on cool surfaces as a mitigation strategy for the SUHI effect in tropical climates. While Kiran's study provides a valuable perspective, the current research underscores the importance of considering a broader range of factors, including landscape metrics and urban planning strategies, in addressing the SUHI effect. This divergence suggests that mitigation strategies may need to be tailored to specific regional and climatic contexts, underscoring the need for further research in this area.

The study also resonates with *Zhou et al*. (2014), who investigated the SUHI effect in China's major cities and identified spatial patterns and drivers. The current study extends this inquiry by identifying similar patterns and drivers in the studied region and suggesting potential mitigation strategies. This comparative analysis underscores the global nature of the SUHI effect and the need for comprehensive, context-specific solutions.

One of the key strengths of this study is the use of a comparative analysis of *LST* variations across different zones over a significant period from 1986 to 2022. This approach has allowed for a comprehensive understanding of the impact of urbanization on temperature rise, particularly in the context of the SUHI effect. The use of mean *LST* as a critical metric has provided a clear and quantifiable measure of the impact of urbanization on temperature.

However, the study is not without its limitations. While useful, reliance on the LST data alone may not capture the full complexity of the SUHI effect, which can influence a range of factors including building materials, vegetation cover, and human activities. Furthermore, the study focuses solely on the Zlatibor main urban area and five surrounding zones, which may limit the generalizability of the findings to other regions or contexts.

In terms of future work, it would be beneficial to incorporate additional variables into the analysis, such as the specific types of urbanization activities in each zone, the types of building materials used, and the extent of vegetation cover. This could provide a more nuanced understanding of the factors contributing to the SUHI effect. Additionally, conducting similar studies in other regions would enhance the generalizability of the findings and contribute to a broader understanding of the impact of urbanization on temperature.

The implications of this study are significant. The findings underscore the urgent need for sustainable urban planning strategies to mitigate the SUHI effect and promote thermal comfort in urban areas. As urbanization continues to increase globally, understanding its impact on temperature and developing strategies to mitigate this effect will be crucial for ensuring the sustainability and liveability of our urban environments.

5. Conclusions

From an urban heat island (UHI) perspective, it is obvious how urbanization contributes to land use changes and increases building density, leading to higher surface air temperatures in urban areas than the in surrounding rural areas. This phenomenon, referred to as the UHI effect, can lead to eco-environmental problems that become more severe with accelerated urbanization.

To better understand the UHI phenomenon, analysing air temperature at urban and rural weather stations and calculating *LST* and *ETa* data from satellite imagery is essential (*Castaldo et al.,* 2015; *Gedzelman et al.*, 2003; *Jiang et al*.,

2019; *Liu* and *Li*, 2018; *Nouri et al.*, 2018; *Yang et al.*, 2018). Remote sensing data and algorithms have been utilized and adapted to examine the UHI scale and effect, and its spatiotemporal evolution features have been analyzed (*Gallo et al.*, 1993; *Gong et al.*, 2008; *Imhoff et al.*, 2010; *Weng et al.*, 2004).

Biosphere-to-biotechnosphere transformation is accelerating increasingly and is accompanied by a disturbance of the ecological balance and the biological basis of the biotechnosphere. Nature has the characteristic of evolution and progress. In contrast, urbanized areas are subject to obsolescence and must be constantly rebuilt. For overly urbanized areas to be sustainable, efforts should be made to maintain the environment's complex geochemical and energetic processes (*Grădinaru et al.*, 2020). The problem is that urban areas are characterised by low biological activity, and very pronounced, generally increasing energy consumption directed toward the immediate satisfaction of human needs. The degradation of the environment is accompanied by the consumption of resources and the emission of polluting substances and energies that damage other natural ecosystems.

It can be concluded that the degree of anthropogenic pressure on nature, taking urbanized areas as an example, is proportional to the difference between the biological characteristics of the original biogeocoenoses and the urban ones that developed later.

Furthermore, in addition to measuring the temperature of a given area, estimates of evapotranspiration derived through remote sensing and global weather datasets offer good information about the existence of UHI. This information is helpful for various applications, including calculating a basin's water budget, evaluating water consumption and crop yield, and monitoring drought conditions.

Understanding the UHI phenomenon is essential, as it can lead to significant eco-environmental problems in urban areas. It also emphasises the significance of using remote sensing data and GIS algorithms to study UHI effects, especially in regions with insufficient weather stations.

This study underscores the significance of the SUHI effect, particularly in urban environments, where it is a critical factor in urban climate change. The SUHI effect, characterized by higher temperatures in urban areas than in surrounding rural ones, is influenced by numerous factors, including urban morphology, land use, and anthropogenic heat. The research also emphasizes the crucial role of green spaces, such as parks and gardens, in mitigating the SUHI effect due to their cooling impact on urban environments. Therefore, the study highlights the importance of comprehensively understanding the SUHI effect and its determinants in developing effective urban climate change mitigation and adaptation strategies. It further underscores the necessity of incorporating green spaces into urban planning and development strategies. The article provides an effective tool for studying the UHI effect, especially in regions with insufficient weather stations. The results provide valuable information on the distribution of

LST in the Zlatibor urban area, which can help study the UHI phenomenon and identify potential areas for implementing UHI mitigation strategies in the area with a significant human development impact on the environment. Finally, research data provide strong evidence of the SUHI effect in Zone 1, with urbanization leading to higher and less variable temperatures than in the surrounding areas. The comparison between 1986 and 2022 clearly shows the significant impact of urbanization on temperature rise over time.

Acknowledgements: The research reported in this paper is supported by Project 451-03-47/2023-01/200091 (Ministry of Science, Technological Development and Innovation of the Republic of Serbia) and Project 1.23/2023 of the Ministry of Defense and the Serbian Army.

References

Almeida, C.R. de, Furst, L., Gonçalves, A., and Teodoro, A.C., 2022: Remote Sensing Image-Based Analysis of the Urban Heat Island Effect in Bragança, Portugal. *Environments - MDPI*, *9*(8), 98. https://doi.org/10.3390/environments9080098

Avdan, U., and *Jovanovska, G.,* 2016: Algorithm for automated mapping of land surface temperature using LANDSAT 8 satellite data. *J. Sensors 2016*, ID 1480307. https://doi.org/10.1155/2016/1480307

Bande, L., Mohamed, M., Asmelash, Y., and Alnuaimi, A., 2022: Residential neighborhood assessment in the city id Al Ain, United Arab Emirates, and the impact on climate change (heat island eddect amalysis). *WIT Trans. Built Environ. 210*. 127–138. https://doi.org/10.2495/ARC220111

Basarin, B., Lukić, T., Bjelajac, D., Micić, T., Stojićević, G., Stamenković, I., Đorđević, J., Đorđević, T., and Matzarakis, A., 2018: Bioclimatic and climatic tourism conditions at Zlatibor mountain (Western Serbia). *Időjárás*, *122*, 321–343. https://doi.org/10.28974/idojaras.2018.3.6

Cao, C., Lee, X., Liu, S., Schultz, N., Xiao, W., Zhang, M., and *Zhao, L.,* 2016: Urban heat islands in China enhanced by haze pollution. *Nat. Commun. 7*. 12509. https://doi.org/10.1038/ncomms12509

Castaldo, V. L., Coccia, V., Cotana, F., Pignatta, G., Pisello, A. L., and *Rossi, F.*, 2015: Thermal-energy analysis of natural "cool" stone aggregates as passive cooling and global warming mitigation technique. *Urban Climate*, *14,* 301–314. https://doi.org/10.1016/j.uclim.2015.05.006

Chen, G., Zhao, L., and *Mochida, A*., 2016: Urban Heat Island simulations in Guangzhou, China, using the coupled WRF/UCM model with a land use map extracted from remote sensing data. *Sustainability 8*(7) 628. https://doi.org/10.3390/su8070628

Cook, M. J. (2014: Atmospheric compensation for a Landsat Land Surface Temperature Product. In RIT Scholar Works. https://doi.org/10.1117/12.2015320

Dimitrijević, M., 1996: Zlatibor, Its Geological Framework . In (Ed. *M.D. Dimitrijević*), Geology of Zlatibor (Special Pu, Vol. 18). Geoinstitute.

Engebretson, C., 2020a: Landsat 8-9 Operational Land Imager (OLI) - Thermal Infrared Sensor (TIRS) Collection 2 Level 2 (L2) Data Format Control Book (DFCB) (Vol. 2, Issue September). Department of the Interior U.S. Geological Survey. Retrieved from https://d9-wret.s3.us-west-2.amazonaws.com/assets/palladium/production/s3fs-public/atoms/files/LSDS-1328_Landsat8-9-OLI-TIRS-C2-L2-DFCB-v6.pdf

Engebretson, C., 2020b: *Landsat Thematic Mapper (TM) Collection 2 (C2) Level 2 (L2) Data Format Control Book (DFCB) Version 4.0*. Department of the Interior U.S. Geological Survey. Retrieved from https://d9-wret.s3.us-west-2.amazonaws.com/assets/palladium/production/s3fs-public/atoms/files/LSDS-1336_Landsat4-5-TM-C2-L2-DFCB-v4.pdf

Esri Inc., 2023: ArcGIS Pro (Version 3.0.3). In *Esri Inc.*

Fardani, I., and *Yosliansyah, M.R*., 2022: Kajian penentuan prioritas ruang terbuka hijau berdasarkan fenomena urban heat island di kota cirebon.. *Jurnal Sains Informasi Geografi*, *5*(2). https://doi.org/10.31314/jsig.v5i2.1708

Gallo, K.P., McNab, A.L., Karl, T.R., Brown, J.F., Hood, J.J., and *Tarpley, J.D*., 1993: The use of NOAA AVHRR data for assessment of the urban heat island effect. *J. Appl. Meteorol. 32*, 899–908. https://doi.org/10.1175/1520-0450(1993)032<0899:TUONAD>2.0.CO;2

Gedzelman, S. D., Austin, S., Cermak, R., Stefano, N., Partridge, S., Quesenberry, S., and *Robinson, D.A*., 2003: Mesoscale aspects of the Urban Heat Island around New York City. *Theor. Appl. Climatol. 75*(1–2), 29–42. https://doi.org/10.1007/s00704-002-0724-2

Gong, A. Du, Xu, J., Zhao, J., and *Li, J.*, 2008: A survey of study method for urban heat island. *J. Nat.Disasters17*(6).

Grădinaru, S.R., Iojă, C. I., Vânău, G.O., and O*nose, D.A.,* 2020: Multi-dimensionality of land transformations: From definition to perspectives on land abandonment. *Carpathian J. Earth Environ. Sci. 15*(1), 161–177. https://doi.org/10.26471/cjees/2020/015/119

Grimm, N.B., Faeth, S.H., Golubiewski, N.E., Redman, C.L., Wu, J., Bai, X., and *Briggs, J.M*., 2008: Global change and the ecology of cities. *Science 319*, 5864. https://doi.org/10.1126/science.1150195

Howard, L., 1833: The Climate of London: Deduced from Meteorological Observations, Made at Different Places in the Neighbourhood of the Metropolis,Vol.1. In IAUC edition.

Imhoff, M.L., Zhang, P., Wolfe, R.E., and *Bounoua, L*., 2010: Remote sensing of the urban heat island effect across biomes in the continental USA. *Remote Sens. Environ. 114*, 504–513. https://doi.org/10.1016/j.rse.2009.10.008

Jiang, P., Liu, X., Zhu, H., and *Li, Y.,* 2019: Features of urban heat Island in mountainous chongqing from a dense surface monitoring network. *Atmosphere*, *10,* 67. https://doi.org/10.3390/atmos10020067

Kiran, K., 2021: Cool surface as urban heat island effect mitigation strategy for tropical climate. Nanyang Technological University. https://doi.org/10.32657/10356/153374

Liu, C., and *Li, Y*., 2018: Spatio-temporal features of urban heat island and its relationship with land use/cover in mountainous city: A case study in Chongqing. *Sustainability 10*(6), 1943. https://doi.org/10.3390/su10061943

Liu, K., Su, H., Zhang, L., Yang, H., Zhang, R., and *Li, X.*, 2015: Analysis of the urban heat Island effect in shijiazhuang, China using satellite and airborne data. *Remote Sensing 7,* 4804–4833. https://doi.org/10.3390/rs70404804

Lješević, M. and *Mihajlović, L.,* 2020: Geomorphological diversity influence on population settlement. *EGU General Assembly 2020*, EGU2020-20838. https://doi.org/10.5194/egusphere-egu2020-20838

Mohajerani, A., Bakaric, J., and J*effrey-Bailey, T.,* 2017: The urban heat island effect, its causes, and mitigation, with reference to the thermal properties of asphalt concrete. *J. Environ. Manage. 197*, 522–538. https://doi.org/10.1016/j.jenvman.2017.03.095

Nouri, A.S., Costa, J.P., Santamouris, M., and *Matzarakis, A*., 2018: Approaches to outdoor thermal comfort thresholds through public space design: A review. *Atmosphere 9*(3), 108. https://doi.org/10.3390/atmos9030108

Novković, I., 2008: Geoheritage of Zlatibor District. *J. Inst.r Nature Conservation of Serbia "Protection of Nature," 58*(1–2), 37–52. https://www.zzps.rs/wp/casopisi_pdf/010/casopis.pdf?script=lat

Pecelj, M., Dordević, A., Pecelj, M.R., Pecelj-Purković, J., Filipović, D., and *Šećerov, V.,* 2017: Biothermal conditions on Mt. Zlatibor based on thermophysiological indices. *Arch. Biol. Sci. 69,* 455–461. https://doi.org/10.2298/ABS151223120P

Pecelj, M., Matzarakis, A., Vujadinović, M., Radovanović, M., Vagić, N., Đurić, D., and *Cvetkovic, M.* (2021: Temporal analysis of urban-suburban pet, mpet and utci indices in belgrade (Serbia). *Atmosphere*, *12*(7), 916. https://doi.org/10.3390/atmos12070916

Pecelj, M., Pecelj, M., Mandic, D., Pecelj, J., Vujadinovic, S., Šecerov, V., Dejan, Š., Gajic, M., and *Milincic, M.,* 2010: Bioclimatic assessment of weather condition for recreation in health resorts. 6th WSEAS Int. Conf. on Cellular and Molecular Biology, Biophys. and Bioeng., BIO'10, 8th WSEAS Int. Conf. on Environ., Ecosystems and Dev., EED'10, Int. Conf. on Biosci. and Bioinformatics, ICBB'10.

Polydoros, A., Cartalis, C., Santamouris, M., and *Kolokotsa, D.,* 2022: Use of landscape metrics for the mitigation of the surface urban heat island effect in Mediterranean cities. *Glob. Urban Heat Island Mitig.* 2022, 95–108. https://doi.org/10.1016/B978-0-323-85539-6.00015-9

Priyadarsini, R., Hien, W.N., and *Wai David, C.K.*, 2008: Microclimatic modeling of the urban thermal environment of Singapore to mitigate urban heat island. *Solar Energy 82*, 727–745. https://doi.org/10.1016/j.solener.2008.02.008

Prostak, C., 2023: Newspaper Map. In *ESRI basemap*. ESRI. Retrieved from https://www.arcgis.com/home/item.html?id=75a3ce8990674a5ebd5b9ab66bdab893

Rao, P., 1972: Remote sensing of urban "heat islands" from an environmental satellite. *Bull. Amer. Meteorol. Soc.*, 647–648.

Republički zavod za statistiku Srbije., 2023: Popisni podaci - eksel tabele. Retrieved from https://www.stat.gov.rs/sr-Latn/oblasti/popis/popis-2011/popisni-podaci-eksel-tabele

RHSS., 1987–2022: Meteorological Yearbook 1. – Climatological Data for [respective year]. Republic Hydrometeorological Service of Serbia. Retrieved from https://www.hidmet.gov.rs/data/meteo_godisnjaci/

Sayler, K. and *Glynn, T.,* 2022: Landsat 4-9 Collection 2 Level-3 Provisional Actual Evapotranspiration Product Guide Version 1.0. Department of the Interior U.S. Geological Survey.

Sayler, K. and *Zanter, K.*, 2021: Landsat 4-7 Collection 2 (C2) Level 2 Science Product (L2SP) Guide Version 4.0 (Vol. 4). Department of the Interior U.S. Geological Survey. Retrieved from https://d9-wret.s3.us-west-2.amazonaws.com/assets/palladium/production/s3fs-public/media/files/LSDS-1618_Landsat-4-7_C2-L2-ScienceProductGuide-v4.pdf

Sayler, K., Zanter, K., and *Glynn, T.,* 2022: Landsat 8-9 Collection 2 (C2) Level 2 Science Product (L2SP) Guide Version 4.0 (Vol. 4, Issue May). Department of the Interior U.S. Geological Survey. Retrieved from https://d9-wret.s3.us-west-2.amazonaws.com/assets/palladium/production/s3fs-public/media/files/LSDS-1619_Landsat-8-9-C2-L2-ScienceProductGuide-v4.pdf

Senay, G.B., 2018: Sattelite Psychrometric Formulation of the Operational Simplified Surface Energy Balance (Ssebop) Model for Quantifying and Mapping Evapotranspiration. *Applied Engineering in Agriculture*, *34*(3) 555–566. https://doi.org/10.13031/aea.12614

Senay, G.B., Bohms, S., Singh, R.K., Gowda, P.H., Velpuri, N.M., Alemu, H., and *Verdin, J.P.*, 2013: Operational Evapotranspiration Mapping Using Remote Sensing and Weather Datasets: A New Parameterization for the SSEB Approach. *J. Amer. Water Res. Assoc. 49*(3). https://doi.org/10.1111/jawr.12057

Senay, G. B., Friedrichs, M., Morton, C., Parrish, G. E. L., Schauer, M., Khand, K., Kagone, S., Boiko, O., and *Huntington, J.,* 2022: Mapping actual evapotranspiration using Landsat for the conterminous United States: Google Earth Engine implementation and assessment of the SSEBop model. *Remote Sens. Environ 275*, 113011. https://doi.org/10.1016/j.rse.2022.113011

Senay, G. B., Parrish, G. E. L., Schauer, M., Friedrichs, M., Khand, K., Boiko, O., Kagone, S., Dittmeier, R., Arab, S., and *Ji, L.*, 2023: Improving the Operational Simplified Surface Energy Balance Evapotranspiration Model Using the Forcing and Normalizing Operation. *Remote Sensing 15,* 260. https://doi.org/10.3390/rs15010260

Stathopoulou, M. and *Cartalis, C.*, 2007: Daytime urban heat islands from Landsat ETM+ and Corine land cover data: An application to major cities in Greece. *Solar Energy*, *81,* 358–368. https://doi.org/10.1016/j.solener.2006.06.014

Stojsavljević, R., Božić, S., Kovačević, M., Živković, M.B., and *Miljković, Đ.*, 2016: Influence of selected climate parameters on tourist traffic of Kopaonik and Zlatibor mountains (Republic of Serbia). *Geographica Pannonica*, *20*(4), 208–219. https://doi.org/10.5937/GeoPan1604208S

Streutker, D.R., 2003: Satellite-measured growth of the urban heat island of Houston, Texas. *Remote Sens. Environ. 85*(3), 282–289. https://doi.org/10.1016/S0034-4257(03)00007-5

Sugiarto, A., Setiawan, B.I., Arif, C., and *Saptomo, S.K.*, 2021: Estimasi Dampak Urban Heat Island terhadap Laju Evapotranspirasi: Studi Kasus di Kota Palembang. *Jurnal Teknik Sipil Dan Lingkungan*, *6*(1). https://doi.org/10.29244/jsil.6.1.23-34

Tan, J., Zheng, Y., Tang, X., Guo, C., Li, L., Song, G., Zhen, X., Yuan, D., Kalkstein, A. J., Li, F., and *Chen, H.* ,2010: The urban heat island and its impact on heat waves and human health in Shanghai. *Int. J. Biometeorol. 54*(1). https://doi.org/10.1007/s00484-009-0256-x

Tang, J., Lan, X., Lian, Y., Zhao, F., and Li, T. (2022: Estimation of Urbanandndash;Rural Land Surface Temperature Difference at Different Elevations in the Qinlingandndash;Daba Mountains Using MODIS and the Random Forest Model. *Int. J. Environ.Res. Publ. Health 19,* 11442. https://doi.org/10.3390/ijerph191811442

Tosic, D. and *Obradovic, D*., 2003: Modern tendencies in developing net of settlements of municipality Smederevo. *Glasnik Srpskog Geografskog Drustva*, *83*(2), 31–44. https://doi.org/10.2298/GSGD0302031T

U.S.G.S. (2015: USGS EarthExplorer. USGS Science for a changing world.

Vakanjac, V.R., Stevanović, Z., Stevanović, A.M., Vakanjac, B., and *Ilić, M.Č.,* 2015: An example of karst catchment delineation for prioritising the protection of an intact natural area. *Environ. Earth Sci. 74,* 7643–7653. https://doi.org/10.1007/s12665-015-4390-y

Vasilescu, A.G., Niță, M.R., and *Pătru-Stupariu, I*., 2022: Methods for identifying the benefits associated with urban green infrastructure at different urban scales. *Carpathian J. Earth Environ. Sci. 17*, 69-80. https://doi.org/10.26471/cjees/2022/017/201

Voogt, J.A. and *Oke, T.R.*, 2003: Thermal remote sensing of urban climates. *Remote Sens. Environ. 86*, 370–384. https://doi.org/10.1016/S0034-4257(03)00079-8

Vukoičić, D., Ristić, D., Milinčić, U., Petrović, D., Mihajlović, L., Božović, S., and *Protić, B.,* 2023: Assessment of the Attractiveness of Natural Resources and Landscapes of the Kopaonik National Park (Serbia): Framework and Importance for Tourism Development. *Polish J. Environ. Studies*, *32*, 281–295. https://doi.org/10.15244/pjoes/152378

Weng, Q., Lu, D., and *Schubring, J.,* 2004: Estimation of land surface temperature-vegetation abundance relationship for urban heat island studies. *Remote Sens. Environ. 89*(4), 467–483. https://doi.org/10.1016/j.rse.2003.11.005

Yang, J., Mohan Kumar, D. llamathy, Pyrgou, A., Chong, A., Santamouris, M., Kolokotsa, D., and *Lee, S.E.,* 2018: Green and cool roofs' urban heat island mitigation potential in tropical climate. *Solar Energy 173,* 597–609. https://doi.org/10.1016/j.solener.2018.08.006

Zhou, D., Zhang, L., Hao, L., Sun, G., Liu, Y., and *Zhu, C.*, 2016: Spatiotemporal trends of urban heat island effect along the urban development intensity gradient in China. *Sci. Total Environ. 544*, 617–626. https://doi.org/10.1016/j.scitotenv.2015.11.168

Zhou, D., Zhao, S., Liu, S., Zhang, L., and *Zhu, C.,* 2014: Surface urban heat island in China's 32 major cities: Spatial patterns and drivers. *Remote Sens. Environ. 152*. 51–61. https://doi.org/10.1016/j.rse.2014.05.017

Zhou, D., Zhao, S., Zhang, L., Sun, G., and *Liu, Y.,* 2015: The footprint of urban heat island effect in China. *Scientific Reports 5*. https://doi.org/10.1038/srep11160

Živanović, V., Pavlović, M., Kovjanić, A., Tošić, D., and Krstić, F. (2021: Concept of polycentricity—the differences between development policies and spatial reality. *J. Geograph. Inst. Jovan Cvijic SASA*, *71*(1), 75–90. https://doi.org/10.2298/IJGI2101075Z